Title	Anisotropic exchange interactions of spin-orbit-integrated states in Sr_2IrO_4
Author(s)	Jin, Hosub; Jeong, Hogyun; Ozaki, Taisuke; Yu, Jaejun
Citation	Physical Review B, 80(7): 075112-1-075112-5
Issue Date	2009-08-13
Type	Journal Article
Text version	publisher
URL	http://hdl.handle.net/10119/10844
Rights	Hosub Jin, Hogyun Jeong, Taisuke Ozaki, and Jaejun Yu, Physical Review B, 80(7), 2009, 075112-1-075112-5. Copyright 2009 by the American Physical Society. http://dx.doi.org/10.1103/PhysRevB.80.075112
Description	

Anisotropic exchange interactions of spin-orbit-integrated states in Sr_2IrO_4

Hosub Jin,[1] Hogyun Jeong,[2] Taisuke Ozaki,[3] and Jaejun Yu[1,4,*]

[1]*Department of Physics and Astronomy and Center for Strongly Correlated Materials Research, Seoul National University, Seoul 151-747, Korea*

[2]*Computational Science and Technology Interdisciplinary Program, Seoul National University, Seoul 151-747, Korea*

[3]*Research Center for Integrated Science, Japan Advanced Institute of Science and Technology, Nomi, Ishikawa 923-1292, Japan*

[4]*Center for Theoretical Physics, Seoul National University, Seoul 151-747, Korea*

We present a microscopic model for the anisotropic exchange interactions in Sr_2IrO_4. A direct construction of Wannier functions from first-principles calculations proves the $j_{eff}=1/2$ character of the spin-orbit integrated states at the Fermi level. An effective j_{eff}-spin Hamiltonian explains the observed weak ferromagnetism and anisotropy of antiferromagnetically ordered magnetic state, which arise naturally from the $j_{eff}=1/2$ state with a rotation of IrO_6 octahedra. It is suggested that Sr_2IrO_4 is a unique class of materials with effective exchange interactions in the spin-orbital Hilbert space.

I. INTRODUCTION

Many of transition metal oxides (TMOs) are antiferromagnetic (AFM) insulators. The simplest model for such Mott insulators is the Hubbard model Hamiltonian,[1] which gives rise to an effective exchange term called superexchange interaction at half-filling. When orbital degrees of freedom are involved, a variety of exchange interactions can occur for a given ionic configuration with different crystal structures. In the case of colossal magnetoresistance manganese oxides, for instance, the superexchange interaction with orbital degeneracy determines complex spin and orbital orderings and, when doped, degenerate e_g orbitals coupled to the lattice via Jahn-Teller interactions become an essential part of the double exchange physics.[2] Sometimes the orbital degrees of freedom via spin-orbit (SO) coupling are responsible for the magnetic anisotropy bound to the crystal environment. When there exists an orbital degeneracy, SO coupling may become a dominant term so that the effective Hamiltonian should involve the full spin-orbital Hilbert space where the ground state must comply with the intersite spin and orbital correlations.[3] A possible dynamic interference between the spin and orbital space was suggested in vanadates.[4] There was a report of a large spin-orbital fluctuations in Mott insulators with t_{2g} orbital degeneracy as a manifestation of quantum entanglement of spin and orbital variables.[5]

Recently we have shown that the electron correlation effect combined with strong SO interactions is responsible for the observed insulating behavior of 5d TMO Sr_2IrO_4.[8] While SO coupling has been considered as a minor perturbation in the description of magnetism,[6] the amount of SO interactions in 5d elements including Ir, for example, is one order of magnitude larger than in the 3d TMO system.[7] Thus the SO coupling is expected to play a significant role in the electronic and magnetic properties of 5d TMO systems. Indeed the manifestation of a novel $j_{eff}=1/2$ Mott ground state in Sr_2IrO_4 was revealed by angle resolved photoemission spectroscopy, optical conductivity, x-ray absorption spectroscopy measurements, and first-principles electronic structure

calculations.[8] Further investigations of the electronic structures of the $Sr_{n+1}Ir_nO_{3n+1}$ (n=1, 2, and ∞) series demonstrated a Mott insulator-metal transition with a change in bandwidth as n increases.[9] The ground state of 5d TMO Sr_2IrO_4 is a Mott insulator in the strong spin-orbit coupling limit. In addition, Sr_2IrO_4 exhibits unusual weak ferromagnetism with reduced Ir magnetic moments.[10–14] To understand such unusual magnetic properties of Sr_2IrO_4, it is necessary to take account of the spin-orbit integrated $j_{eff}=1/2$ state.

In this paper, we introduce a prototype model of spin-orbit-integrated magnetism realized in Sr_2IrO_4. From a tight-binding (TB) analysis based on first-principles calculations, we show that the $j_{eff}=1/2$ character of the spin-orbit-integrated state remains robust even in the presence of on-site Coulomb interactions. A direct construction of Wannier functions from first-principles calculations proves the $j_{eff}=1/2$ character at the Fermi level. An effective exchange Hamiltonian with no $S=1/2$ but $j_{eff}=1/2$ is obtained starting from a $j_{eff}=1/2$ Hubbard model. The origin of anisotropic magnetic exchange interactions is discussed in connection with an extraordinary character of the ground state. The presence of spin-orbit-integrated state with strong SO interactions in Sr_2IrO_4 can make Ir 5d oxides a unique class of materials for the study of effective exchange interactions in the full spin-orbital Hilbert space.

II. SPIN-ORIBT-INTEGRATED ELECTRONIC STATES

A. LDA+SO+U band structure

Since both on-site Coulomb interactions (U) and SO couplings are expected to be important in the description of Ir 5d states, we examined the effect of on-site U and SO couplings separately and simultaneously on the electronic structure of Sr_2IrO_4. To identify the role of each term and the interplay between them, we carried out density-functional-theory (DFT) calculations within the local-density approximation (LDA), LDA including the SO coupling (LDA+SO), and LDA+U including the SO coupling (LDA+SO+U). We cal-

culated total energies and electronic band structures of Sr_2IrO_4 for the structural parameters as obtained from the neutron powder diffraction data at 10 K,[15] which has a K_2NiF_4-type layered perovskite structure with the symmetry of the space group $I4_1/acd$ reduced from $I4/mmm$, where IrO_6 octahedra are rotated by about $11°$ around the c axis of the unit cell. For the calculations, we used the DFT code, OPENMX,[16] based on the linear-combination-of-pseudoatomic-orbital method,[17] where both the LDA+U method[18] and the SO couplings were included via a relativistic j-dependent pseudopotential scheme in the noncollinear DFT formalism.[19–21] Double valence and single polarization orbitals were used as a basis set, which were generated by a confinement potential scheme with cutoff radii of 8.0, 7.0, and 5.0 a.u. for Sr, Ir, and O atoms, respectively. We used a $(6 \times 6 \times 4)$ **k**-point grid for the k-space integration.

Calculated LDA, LDA+SO, and LDA+SO+U band structures were presented in the previous work[8] where the results of the LDA+SO+U band structures of Sr_2IrO_4 are well compared with those of angle resolved photoemission spectroscopy experiments. The LDA bands near the Fermi level (E_F), as shown in Fig. 2(a) in Ref. 8, are almost identical to those of Sr_2RhO_4,[22] which can be expected from the same d^5 configuration of Rh^{4+} and Ir^{4+} and the same structural distortions, i.e., the rotations of RhO_6 and IrO_6 octahedra. The hybridization of d_{xy} and $d_{x^2-y^2}$ due to the rotation of IrO_6 octahedra pushes the d_{xy} band below E_F, similarly to the case of Sr_2RhO_4. Indeed the LDA Fermi surface of Sr_2IrO_4 was found to be basically the same as that of Sr_2RhO_4.[22]

In the LDA band structure, the contributions of d_{xy} components above E_F are strongly suppressed relative to those of d_{yz} and d_{zx} states, whereas the Ir 5d bands ranging from -2.5 to 0.5 eV are still dominated by the t_{2g} orbitals with a small admixture of $d_{x^2-y^2}$. On the other hand, however, when the SO coupling is included, a significant change in the wave function character occurs so that all three t_{2g} orbital components are almost equally distributed in the LDA+SO band structure. This change arises from the SO interactions acting on the t_{2g} manifold, which mixes up the d_{xy}, d_{yz}, and d_{zx} orbitals. This qualitative change in the wave function character is an essence of the SO coupling action, which is related to the novel nature of the SO-integrated insulating ground state.

As shown in the inset of Fig. 1, an effective $U=2$ eV opens up a gap in the LDA+SO+U band structure and gives rise to the nondispersive and parallel features of "upper" and "lower" Hubbard bands of the SO-integrated states, which are in excellent agreement with experimental observations.[8] It is remarkable to obtain an insulating ground state for the intermediate value of U, which is smaller than the bandwidth of the t_{2g} manifold and the conventional U values of 3d TMOs. On the other hand, however, when we performed LDA+U calculations without the SO coupling, the on-site Coulomb interaction became *ineffective* due to the threefold degeneracy of the Ir t_{2g} manifold crossing E_F.[23] Unless the degeneracy is broken, each band remains partially filled being far from the Mott instability. In our noncollinear DFT calculations, the SO coupling terms were solved in a completely nonperturbative way, whereas the Coulomb correlation effects were treated via the LDA+U method.
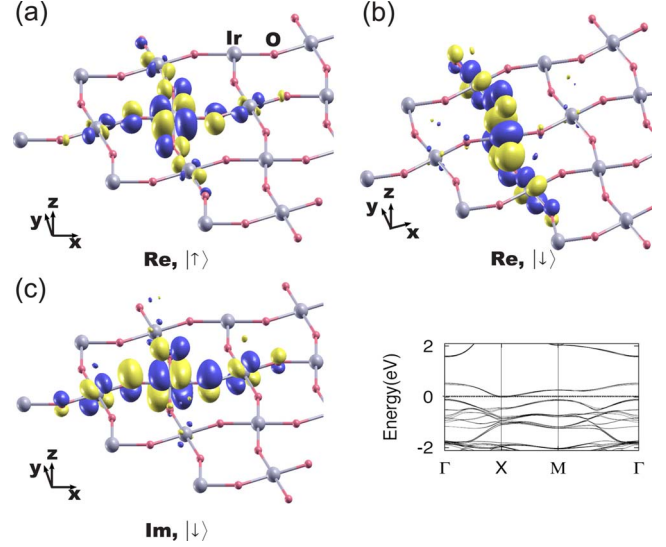

FIG. 1. (Color online) Calculated Wannier functions of the $|j_{eff}=1/2,+1/2\rangle$ state: (a) the real part of up-spin $|\uparrow\rangle$ component, (b) the real part of the down-spin $|\downarrow\rangle$ component, and (c) the imaginary part of the down-spin $|\downarrow\rangle$ component. Blue (dark gray) and yellow (light gray) colors in the Wannier function represent negative and positive values, respectively. The inset shows the LDA +SO+U band structure near $E_F=0$ eV, emphasizing the upper and lower Hubbard bands of the $|j_{eff}=1/2,m\rangle$ band above and below E_F, respectively.

In order to examine the nature of the SO-integrated state, we constructed Wannier functions which can identify the orbital shape and bonding character of the upper and lower Hubbard bands of the SO-integrated states, as shown in the inset of Fig. 1. The Wannier functions were calculated for the t_{2g} manifold by employing the projection scheme.[24] The Wannier function illustrated in Fig. 1 corresponds to the single band above E_F of LDA+SO+U bands. As listed in Table I, the overall shape of the calculated Wannier function of Fig. 1 matches closely to the ideal $j_{eff}=1/2$ state,

$$\left| j_{eff} = \frac{1}{2}, \pm \frac{1}{2} \right\rangle = \mp \frac{1}{\sqrt{3}} [|d_{xy}\rangle| \pm \rangle \pm (|d_{yz}\rangle \pm i|d_{zx}\rangle)| \mp \rangle],$$

(1)

where $|\pm\rangle$ represent for the up-spin $|\uparrow\rangle$ and down-spin $|\downarrow\rangle$ states, respectively. The agreement of its orbital components

TABLE I. Coefficients of the Wannier functions illustrated in Fig. 1: only the coefficients from the center Ir are listed.

		Up spin		Down spin	
		Re	Im	Re	Im
Ir	d_{z^2}	0.00009	0.00009	0.00002	0.00001
	$d_{x^2-y^2}$	−0.09044	−0.01212	−0.00024	0.00016
	d_{xy}	0.32738	0.00000	0.00115	−0.00009
	d_{yz}	−0.00203	−0.00001	0.44105	0.05527
	d_{zx}	−0.00018	0.00183	−0.05450	0.44212

and their relative phases between the ideal state and the calculated Wannier function is another proof of the SO-integrated $j_{eff}=1/2$ state. Here, for the sake of simplicity in the presentation, we chose a self-consistent solution with the spin quantization axis parallel to the z axis.

B. Tight-binding model

The physics of the LDA+SO+U results can be captured by a multiband Hubbard model for the t_{2g} bands including the SO coupling term. The TB bands for the t_{2g} manifold can be described by

$$\mathcal{H}_0 = \sum_{\langle ij \rangle \alpha\beta\sigma} t_{ij}^{\alpha\beta} c_{i\alpha\sigma}^\dagger c_{j\beta\sigma} + \sum_{i,a=d_{xy}} \Delta_t c_{ia\sigma}^\dagger c_{ja\sigma} + \lambda_{SO} \sum_i \mathbf{L}_i \cdot \mathbf{S}_i,$$
(2)

where $\langle ij \rangle$ runs over the nearest-neighbor pairs of sites i and j in the two-dimensional square lattice consisting of Ir ions, α and β are indices for t_{2g} orbitals, i.e., $\{d_{xy}, d_{yz}, d_{zx}\}$, $t_{ij}^{\alpha\beta}$ is a hopping integral between $|i\alpha\rangle$ and $|j\beta\rangle$, Δ_t is a tetragonal crystal field splitting, i.e., an on-site energy difference of the d_{xy} orbital relative to d_{yz} and d_{zx}, and λ_{SO} is the SO coupling parameter. In a simple square lattice of Ir ions, $t_{ij}^{\alpha\beta}$ becomes a nonzero constant t_0 only for $(\alpha,\beta)=(d_{xy},d_{xy})=(d_{zx},d_{zx})$ with $j=i+\hat{x}$ and so on.

Starting from a set of $\{\langle n_{i\tau\alpha\sigma} \rangle\}$ as mean-field parameters, we could obtain a self-consistent mean-field Hamiltonian within the t_{2g} subspace by $\mathcal{H}_{t_{2g}} = \Sigma_\mathbf{k} C_\mathbf{k}^\dagger \hat{\mathcal{T}}(\mathbf{k}) C_\mathbf{k}$, where $C_\mathbf{k}$ has 12 components of $\{c_{\mathbf{k}\tau\alpha\sigma} | \tau=A,B; \alpha=d_{xy},d_{yz},d_{zx}; \sigma=\uparrow,\downarrow\}$. Here the site indices $\tau=A,B$ are for the two inequivalent Ir sites. By choosing the basis in order of $(c_{Ad_{xy}\uparrow}, c_{Ad_{yz}\downarrow}, c_{Ad_{zx}\uparrow}, [A \to B], [\uparrow \leftrightarrow \downarrow])$, we can find a block-diagonal $12 \times 12 \hat{\mathcal{T}}(\mathbf{k})$ matrix,

$$\hat{\mathcal{T}}(\mathbf{k}) = \begin{pmatrix} \mathbf{D}_I^A & \mathbf{O}(\mathbf{k}) & 0 & 0 \\ \mathbf{O}^\dagger(\mathbf{k}) & \mathbf{D}_I^B & 0 & 0 \\ 0 & 0 & \mathbf{D}_{II}^A & \mathbf{O}(\mathbf{k}) \\ 0 & 0 & \mathbf{O}^\dagger(\mathbf{k}) & \mathbf{D}_{II}^B \end{pmatrix}.$$
(3)

Here the hopping integrals contribute to $\mathbf{O}(\mathbf{k})$,

$$\mathbf{O}(\mathbf{k}) = e^{-i(k_x+k_y/2)} \begin{pmatrix} -4t_0\gamma_{1\mathbf{k}} & 0 & 0 \\ 0 & -2t_0\gamma_{2\mathbf{k}} & 0 \\ 0 & 0 & -2t_0\gamma_{3\mathbf{k}} \end{pmatrix},$$
(4)

where the nonzero hopping terms of $t_0=t_{d_{xy}}=t_{d_{yz}}=t_{d_{zx}}$ lead to the dispersions $\gamma_{1\mathbf{k}}=\cos(k_x/2)\cos(k_y/2)$, $\gamma_{2\mathbf{k}}=\cos[(k_x+k_y)/2]$, and $\gamma_{3\mathbf{k}}=\cos[(k_x-k_y)/2]$ for d_{xy}, d_{yz}, and d_{zx} bands, respectively. The on-site Coulomb interaction U and the SO coupling λ_{SO} contribute to the diagonal term,

$$\mathbf{D}_I^\tau = \begin{pmatrix} \Delta_t + e_1\gamma_{1\mathbf{k}}^2 - U\bar{n}_{\tau d_{xy}\uparrow} & \lambda_{SO}/2 & -i\lambda_{SO}/2 \\ \lambda_{SO}/2 & -U\bar{n}_{\tau d_{yz}\downarrow} & -i\lambda_{SO}/2 \\ \iota\lambda_{SO}/2 & i\lambda_{SO}/2 & -U\bar{n}_{\tau d_{zx}\downarrow} \end{pmatrix},$$
(5)

and $\mathbf{D}_{II}^\tau$ is a time-reversal partner of $\mathbf{D}_I^\tau$.

Despite of a large cubic crystal field splitting due to $\Delta_c \approx 5$ eV between t_{2g} and e_g, there is a significant hybridiza-
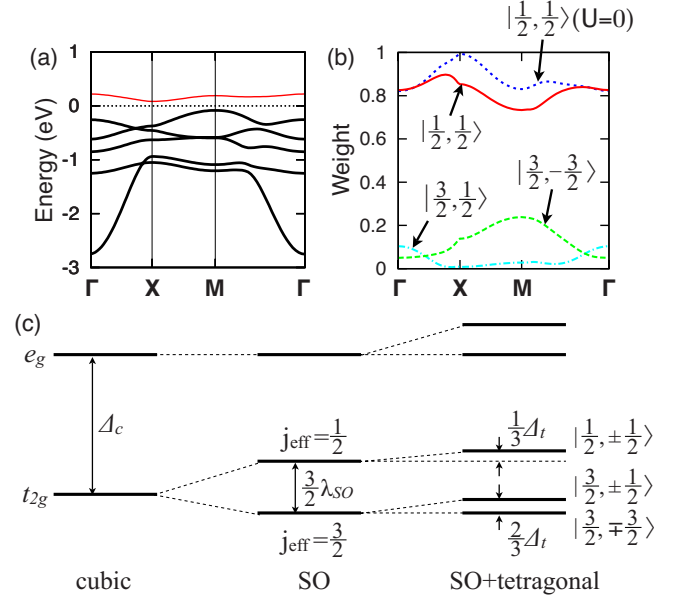

FIG. 2. (Color online) (a) Tight-binding band structure with $(\lambda_{SO}, U)=(0.4$ eV, 2.0 eV), which is well compared with the LDA+SO+U band structure of Figs. 1(c) and 1(b) the decomposition of the upper Hubbard band wave function [marked by a thin (red) solid line in (a)] into the $\{|j_{eff}, m_j\rangle\}$ basis, where the dotted line represents a $|\frac{1}{2}, \frac{1}{2}\rangle$ component with $U=0$, and (c) a schematic energy diagram of the t_{2g} manifold in the atomic limit. Due to the large crystal field splitting by Δ_c, the t_{2g} levels can be mapped into the effective $l_{eff}=1$ states where the tetragonal field splitting by Δ_t is relatively insignificant.

tion of d_{xy} and $d_{x^2-y^2}$ due to the rotation of IrO$_6$ octahedra. In order to describe both LDA and LDA+SO band structures properly, the contribution of the $d_{x^2-y^2}$ admixture is necessary to be included as a $\mathbf{k}$-dependent energy $\Delta\varepsilon_{\mathbf{k}d_{xy}}$ for the d_{xy} band: $\Delta\varepsilon_{\mathbf{k}d_{xy}}=e_1\gamma_{1\mathbf{k}}^2$. The best fit to the LDA bands was obtained by a set of parameters: $\Delta_t=0.15$ eV, $t_0=0.35$ eV, and $e_1=-1.5$ eV.

The solutions of our TB model including both SO coupling λ_{SO} and on-site Coulomb interaction U with different sets of parameters $(\lambda_{SO}, U)=(0,0)$, $(0.4$ eV, $0)$, and $(0.4$ eV, 2.0 eV) reproduce well the t_{2g} manifold of the LDA, LDA+SO, and LDA+SO+U bands, respectively. The self-consistent solution for $(\lambda_{SO}, U)=(0.4$ eV, 2.0 eV) is shown in Fig. 2(a), which corresponds to the LDA+SO+U bands of the inset of Fig. 1.

In addition to the large crystal field splitting between e_g and t_{2g}, the t_{2g} manifold splits further into doubly degenerate $j_{eff}=1/2$ and quadruply degenerate $j_{eff}=3/2$ states due to SO coupling. The small tetragonal crystal field does not affect this configuration. A schematic energy level diagram shown in Fig. 2(c) was confirmed by the LDA and LDA+SO energy levels at the X point,[8] where the off-diagonal hopping matrix $\mathbf{O}(\mathbf{k})$ in the TB model becomes zero. Even though the nonzero hopping terms away from X point may disturb the atomic picture, the SO coupling retains the anticrossing between those levels which transform according to the same irreducible representation.[25] Consequently, the effective bandwidth of the half-filled $j_{eff}=1/2$ band becomes smaller

than the modest value of on-site U. The decomposition of the upper Hubbard band wave function into the $\{|j_{eff}, m_j\rangle\}$ basis clearly demonstrates the robustness of its $j_{eff} = 1/2$ character as shown in Fig. 2(b), whereas the $j_{eff} = 1/2$ weight for $U = 2$ eV is slightly reduced from that of $U = 0$. Therefore it is reasonable to consider an effective Hamiltonian based on the $j_{eff} = 1/2$ single-band Hubbard model instead of the conventional $S = 1/2$ model,

$$\mathcal{H} = \sum_{\langle ij \rangle mm'} \bar{t}_{mm'}^{ij} d_{im}^\dagger d_{jm'} + \bar{U} \sum_i n_{di+1/2} n_{di-1/2}, \quad (6)$$

where d_{im} represents for the $|j_{eff} = 1/2, m\rangle$ state at the site i with $m, m' = \pm 1/2$ and $n_{dim} = d_{im}^\dagger d_{im}$. $\bar{t}_{mm'}^{ij}$ and $\bar{U}$ are effective hopping and on-site interaction parameters, respectively.

III. ANISOTROPIC EXCHANGE INTERACTIONS

A. Effective exchange Hamiltonian

The $j_{eff} = 1/2$ single-band Hubbard model has an interesting feature in $\bar{t}_{mm'}^{ij}$, which originates from a peculiar nature of the spin-orbit integrated state in Sr_2IrO_4. In the strong SO coupling limit, the orbital wave functions of the $|j_{eff} = 1/2, m\rangle$ state of Eq. (1) consist of the cubic harmonics with respect to the local coordinate axes. The rotation of the IrO_6 octahedron results in a rotation of the $|j_{eff} = 1/2, m\rangle$ state at each site i, thereby generating a spin-dependent hopping term. In Sr_2IrO_4, where the IrO_6 octahedron is rotated by an angle $\theta \approx 11°$ about the c axis, the effective hopping matrix $\bar{t}_{mm'}^{ij}$ can be represented in terms of Pauli matrices by $\mathbf{t}^{ij} = \bar{t}_0 \mathbf{1} + i\bar{t}_1 \sigma_z$, where $\bar{t}_0$ and $\bar{t}_1$ for $(ij) = \hat{x}$ or $\hat{y}$ become

$$\bar{t}_0^{\hat{x}/\hat{y}} = \frac{2t_0}{3} \cos\theta (2\cos^4\theta - 1), \quad (7)$$

$$\bar{t}_1^{\hat{x}/\hat{y}} = \frac{2t_0}{3} \sin\theta (2\sin^4\theta - 1). \quad (8)$$

At half-filling, an effective j_{eff}-spin Hamiltonian can be derived from the $j_{eff} = 1/2$ single-band Hubbard model of Eq. (6),

$$\mathcal{H}_{spin} = \sum_{\langle ij \rangle} [I_0 \mathbf{J}_i \cdot \mathbf{J}_j + I_1 J_{zi} J_{zj} + \mathbf{D}_{ij} \cdot \mathbf{J}_i \times \mathbf{J}_j], \quad (9)$$

where $I_0 = 4(\bar{t}_0^2 - \bar{t}_1^2)/\bar{U}$, $I_1 = 8\bar{t}_1^2/\bar{U}$, and $\mathbf{D}_{ij} = D_z \hat{z}$ with $D_z = 8\bar{t}_0 \bar{t}_1/\bar{U}$. The first term is a conventional Heisenberg form of superexchange with the coupling constant I_0. The second and third terms are pseudodipolar and Dzyaloshinkii-Moriya (DM) antisymmetric exchange interactions, which originate from the pure imaginary hopping matrix element $i\bar{t}_1$ between the neighboring $|j_{eff} = 1/2, m\rangle$ states of rotated IrO_6 octahedra.

B. Comparison with LDA+SO+U results

From our LDA+SO+U calculations, the magnetic configuration of the insulating ground state was determined to be a canted AFM state with the ab plane as an easy plane. We
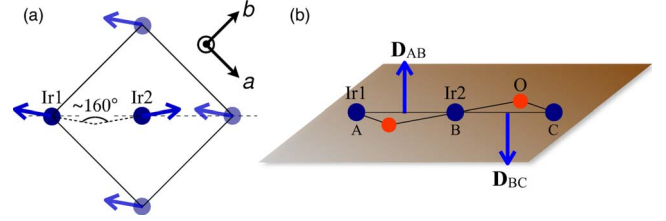

FIG. 3. (Color online) (a) Magnetic configuration and (b) DM vectors of the calculated LDA+SO+U ground state of Sr_2IrO_4. Blue (gray) arrows in (a) represent a noncollinear ordering of the local Ir moments, consisting of both spin and orbital components, in a canted AFM configuration. The DM vectors, $\mathbf{D}_{AB}$ and $\mathbf{D}_{BC}$, in (b) are aligned along the c axis with alternating signs and consistent with the DM rule.

found no preferred direction within the ab plane. As illustrated in Fig. 3(a), there are two inequivalent Ir sites, i.e., Ir1 and Ir2 within the $\sqrt{2} \times \sqrt{2}$ unit cell. It is found that the magnetic moment at each Ir site is $0.36\mu_B$ and both spin $(0.10\mu_B)$ and orbital $(0.26\mu_B)$ moments are parallel to each other. In addition, AFM moments are canted with the canting moment $0.063\mu_B$, which is comparable to the single crystal measurement.[12]

According to the rule by Dzyaloshinkii and Moriya,[6] the direction of the vector $\mathbf{D}_{ij}$ in Sr_2IrO_4 should point to the c axis due to a mirror plane containing Ir1-O-Ir2, as illustrated in Fig. 3(b). The directions of $\mathbf{D}_{ij}$ can be represented by $\mathbf{D}_{AB} = -\mathbf{D}_{BC} = (0, 0, d_c)$ when considering the inversion symmetry at site B, which gives the consistent results as the $j_{eff} = 1/2$ Hamiltonian of Eq. (9). From the LDA+SO+U calculations, it is concluded that the DM interaction is responsible for the magnetic anisotropy of Sr_2IrO_4 with the ab plane as an easy plane but isotropic within the ab plane, whereas the single-ion anisotropy term has a negligible contribution. Contrary to the La_2CuO_4,[26] which has no single-ion anisotropy due to the $S = 1/2$ ground state, the absence of the ab-plane anisotropy in Sr_2IrO_4 is attributed to the tetragonal symmetry.

From the effective exchange Hamiltonian of Eq. (9), the ratio of D_z/I_0, which determines the spin canting angle, becomes $|D_z/I_0| \approx \tan 2\theta$ for small θ. In the strong SO coupling limit, the canting angle increases close to the rotation angle of IrO_6 octahedra. We can estimate the magnitude of $\mathbf{D}_{ij}$ to be $|\mathbf{D}| \approx 3.8$ meV assuming the intersite superexchange interaction $J \approx 10$ meV. This enormous DM interaction may well be related to the peculiar nature of the $j_{eff} = 1/2$ state. Contrary to the $S = 1/2$ counterpart of La_2CuO_4,[26] the $j_{eff} = 1/2$ state has an open shell of the $l = 1$ orbital where the nonperturbative ground state of $j_{eff} = 1/2$ spin-orbit coupled state contributes to the DM term. Although the small magnetic moment of Ir observed in experiments was attributed to the effective moment the $j_{eff} = 1/2$ state, one can expect possible contributions from the $j = 1/2$ quantum fluctuation. Nevertheless, since $j_{eff} = 1/2$ state is an eigenstate of the fictitious angular moment $\mathbf{J}_{eff} = \mathbf{L}_{eff} + \mathbf{S} = -\mathbf{L} + \mathbf{S}$, the orbital contribution to the magnetic moment needs a careful interpretation.[8]

IV. CONCLUSIONS

In summary, we presented the effective $j_{\rm eff}$-spin model Hamiltonian for Sr_2IrO_4. The strong SO interaction combined with the large crystal field splitting in $5d$ TMOs introduces a unique form of the spin-orbit integrated band state at $E_{\rm F}$, leading to an effective insulating ground state of $j_{\rm eff} = 1/2$ quantum magnet. The observed weak ferromagnetism is understood by the DM anisotropic exchange interaction where the effective exchange interactions arise from the full spin-orbital Hilbert space. We hope that our prototype model of the spin-orbit integrated magnetism is useful for the study of various spin-orbit entangled physics. By taking an analogy of the high T_c superconductors as a doped $S = 1/2$ quantum magnet, it will be interesting to observe a doped $j = 1/2$ quantum magnet as a spin-orbit integrated correlated electron system.

ACKNOWLEDGMENTS

---

*Corresponding author; jyu@snu.ac.kr

[1] J. Hubbard, Proc. R. Soc. London, Ser. A **276**, 238 (1963).

[2] S. Maekawa, T. Tohyama, S. E. Barnes, S. Ishihara, W. Koshibae, and G. Khaliullin, *Physics of Transition Metal Oxides*, Springer Series in Solid State Sciences Vol. 144 (Springer-Verlag, Berlin, 2004).

[3] G. Jackeli and G. Khaliullin, Phys. Rev. Lett. **102**, 017205 (2009).

[4] J.-S. Zhou, J. B. Goodenough, J.-Q. Yan, and Y. Ren, Phys. Rev. Lett. **99**, 156401 (2007).

[5] A. M. Oleś, P. Horsch, L. F. Feiner, and G. Khaliullin, Phys. Rev. Lett. **96**, 147205 (2006).

[6] K. Yosida, *Theory of Magnetism*, Springer Series in Solid State Sciences Vol. 122 (Springer-Verlag, Berlin, 1996).

[7] L. F. Mattheiss, Phys. Rev. B **13**, 2433 (1976).

[8] B. J. Kim *et al.*, Phys. Rev. Lett. **101**, 076402 (2008).

[9] S. J. Moon *et al.*, Phys. Rev. Lett. **101**, 226402 (2008).

[10] M. K. Crawford, M. A. Subramanian, R. L. Harlow, J. A. Fernandez-Baca, Z. R. Wang, and D. C. Johnston, Phys. Rev. B **49**, 9198 (1994).

[11] T. Shimura, Y. Inaguma, T. Nakamura, M. Itoh, and Y. Morii, Phys. Rev. B **52**, 9143 (1995).

[12] G. Cao, J. Bolivar, S. McCall, J. E. Crow, and R. P. Guertin, Phys. Rev. B **57**, R11039 (1998).

[13] N. S. Kini, A. M. Strydom, H. S. Jeevan, C. Geibel, and S. Ramakrishnan, J. Phys.: Condens. Matter **18**, 8205 (2006).

[14] S. J. Moon *et al.*, Phys. Rev. B **74**, 113104 (2006).

[15] Q. Huang, J. L. Soubeyroux, O. Chmaissem, I. N. Sora, A. Santoro, R. J. Cava, J. J. Krajewski, and W. F. Peck, Jr., J. Solid State Chem. **112**, 355 (1994).

[16] The DFT code, OPENMX, is available at the web site http://www.openmx-square.org in the constitution of the GNU General Public License.

[17] T. Ozaki, Phys. Rev. B **67**, 155108 (2003).

[18] M. J. Han, T. Ozaki, and J. Yu, Phys. Rev. B **73**, 045110 (2006).

[19] A. H. MacDonald and S. H. Vosko, J. Phys. C **12**, 2977 (1979).

[20] G. B. Bachelet, D. R. Hamann, and M. Schlüter, Phys. Rev. B **26**, 4199 (1982).

[21] G. Theurich and N. A. Hill, Phys. Rev. B **64**, 073106 (2001).

[22] B. J. Kim, J. Yu, H. Koh, I. Nagai, S. I. Ikeda, S.-J. Oh, and C. Kim, Phys. Rev. Lett. **97**, 106401 (2006).

[23] We have tried an unphysically large $U = 6$ eV in LDA+U without the SO coupling and then obtained an insulating ground state with a large spin and orbital polarization, which may lead to a lattice distortion.

[24] V. I. Anisimov *et al.*, Phys. Rev. B **71**, 125119 (2005).

[25] R. Winkler, *Spin-Orbit Coupling Effects in Two-Dimensional Electron and Hole Systems* (Springer-Verlag, Berlin, 2003).

[26] S.-W. Cheong, J. D. Thompson, and Z. Fisk, Phys. Rev. B **39**, 4395 (1989).